Improved Accuracy and Efficiency of Flood Inundation Mapping of Low-, Medium-, and High-Flow Events Using the AutoRoute Model

Michael L. Follum[1,2], Ricardo Vera[3], Ahmad A. Tavakoly[1,4], and Joseph L. Gutenson[1,5]

[1]Coastal and Hydraulics Laboratory, Engineer Research and Development Center, 3909 Halls Ferry Road, Vicksburg, MS 39180, USA
[2]Wyoming Area Office, U.S. Bureau of Reclamation, 705 Pendell Blvd., Mills, WY 82644, USA.
[3]Cold Regions Research and Engineering Laboratory, Engineer Research and Development Center, 72 Lyme Road, Hanover, NH 03755, USA
[4]Earth System Science Interdisciplinary Center, University of Maryland, College Park, MD 20740, USA
[5]National Water Center, National Oceanic and Atmospheric Administration, 205 Hackberry Ln, Tuscaloosa, AL 35401, USA

Correspondence to: Michael L. Follum (follumm@gmail.com)

Summary of Author Response

We would like to thank the editor (ED) and referees (R1, R2, and R3) for their comments and suggestions. We appreciate all their insights, which we believe improved the manuscript. In this document we respond to each comment and describe the associated changes to the manuscript. All line and page numbers refer to the manuscript with no changes marked.

ED – General Issue #1. Accuracy comparison between the old post-processing procedure and the updated post-processing scripts.

We agree with the editor that including a comparison between the previous post-processing procedure (GISPP) and the updated post-processing procedure (ARPP) will improve the paper. We have modified the beginning of Section 4.1 (Lines 236-249) to incorporate a test between the GISPP and ARPP. The results (F and E statistics) are now shown in Table 3. In several locations we now also discuss the improvement in accuracy using the ARPP (Lines 16, 359-366).

ED – General Issue #2. Parameter sensitivity analyses on post-processing parameters.

Lines 224-233 and Figure 4 have now been added to provide a parameter sensitivity test on the user-defined α value, which in ARPP controls the influence that each stream cell has on flooding the surrounding cells.

R1 - General Issue #1. More details should be given on how the parameters of the exponential channel profile is generated from a given top width.

We agree with the reviewer and a section has been added that describes the method and parameters required for AutoRoute to estimate a bathymetric profile (Lines 111-121). Figure 1 has also been modified to better explain the methods for bathymetric estimation within AutoRoute.

R1 - General Issue #2. The authors should at least list a few possible reasons why these outliers occur (question associated with Figure 2).

Outliers in the flood depth calculation exist for several reasons, many of them are listed in Lines 69-73. Lines 169-170 were also added to address the source of outliers. We agree with the reviewer that the existence of depth outliers needs to be resolved and this topic is listed as an avenue for future research (Lines 387-389).

R1 - General Issue #3. Does the lidar DEM share the same flat bottom width as the 9-meter NED? Also, another figure showing the difference between the ned-simulated inundation extent and the lidar-simulated extent might be desirable. Two subplots of the raw DEMs for the same spot can be added on the left as the reference to give readers an idea about the level of land surface details different-resolution DEMs contains.

We agree with the reviewer that analysing the effects of different elevation resolution on flood inundation accuracy is important and we now include Lines 291-295 to stress the importance of quality elevation data. Several papers have addressed the issue of elevation resolution and accuracy when using hydraulic models (a few are now listed in Lines 293-294). However, none of these research efforts have included the AutoRoute model and therefore we have included analysis of elevation and bathymetry data as a future research effort (Lines and 385-386).

In Section 4.2 and Figures 8 and 9 we utilize 3-m elevation data, which is processed from LiDar. We have used raw LiDar in previous studies and have found the spikes in the data make it difficult to use within the AutoRoute model (numerous outliers related to R1 - General Issue #2). To specifically answer the reviewer's question, both the 9- and 3-m elevation datasets used in this study have "flat" bottoms over the water surface. Depending on the (post)processing of other LiDar datasets, the water surface may or may not be flat. In order to keep the scope of the paper limited and to minimize the number and size of the Figures, we have included several references to studies that have analysed various elevation datasets (Lines 293-294) in-lieu of adding/modifying Figures. We reiterate that we do see the value of using various elevation datasets but believe that this would be better served in a future research effort.

R2 – General Issue #1. A figure providing the geographic locations of all the sites used in the study on a US map to provide more context to the readers outside the United States.

We agree with the reviewer and now included Figure 3 (also see Line 184), which shows the test site locations on a US map.

R3 – General Issue #1. Accuracy comparison between the old post-processing procedure and the updated post-processing scripts.

We agree with the reviewer that including a comparison between the previous post-processing procedure (GISPP) and the updated post-processing procedure (ARPP) will improve the paper. We have modified the beginning of Section 4.1 (Lines 236-249) to incorporate a test between the GISPP and ARPP. The results (F and E statistics) are now shown in Table 3. In several locations we now also discuss the improvement in accuracy using the ARPP (Lines 16, 359-366).

R3 – General Issue #2. Why not presenting a tool that incorporates the whole AutoRoute post-processing workflow, but only a script is specifically created for weight calculation?

The only post-processing component not included within ARPP is the conversion from raster format to flood inundation polygons (for which one can use ArcGIS or GDAL) (Line 163). The reason we have not included the conversion from raster to polygon within ARPP is that this post-processing step is often not utilized (mobility models typically utilize raster-based inputs). In the next update to ARPP we will likely provide the option to convert directly to shapefile polygons using ARPP.

R3 – General Issue #3. Parameter sensitivity analyses on post-processing parameters.

Lines 224-233 and Figure 4 have now been added to provide a parameter sensitivity test on the user-defined α value, which in ARPP controls the influence that each stream cell has on flooding the surrounding cells.

R3 – General Issue #4. Utilize higher-elevation data.

We agree with the reviewer that analysing the effects of different elevation resolution on flood inundation accuracy is important and we now include Lines 291-295 to stress the importance of quality elevation data. Several papers have addressed the issue of elevation resolution and accuracy when using hydraulic models (a few are now listed in Lines 293-294). However, none of these research efforts have included the AutoRoute model and therefore we have included analysis of elevation and bathymetry data as a future research effort (Lines and 385-386).

In Section 4.2 and Figures 8 and 9 we utilize 3-m elevation data, which is processed from LiDar. We have used raw LiDar in previous studies and have found the spikes in the data make it difficult to use within the AutoRoute model (numerous flood depth outliers at the stream cells), however these errors associated with raw LiDar would not be unique to AutoRoute. In order to keep the scope of the paper limited and to minimize the number and size of the Figures, we have included several references to studies that have analysed various elevation datasets (Lines 293-294) in-lieu of simulating more results using even higher resolution elevation data.. We reiterate that we do see the value of using various elevation datasets but believe that this would be better served in a future research effort.

R3 – General Issue #5. was the computational cost reduction (described in Section 4.3) purely a result of the use of GDAL I/O functions (L477)?

The use of GDAL I/O did reduce the computation cost of running AutoRoute (Lines 332-335). However, the reduction of computation cost of the post-processing (the majority of total computational savings, Lines 332-338) is due to the use of the ARPP method outlined in Section 2.2 instead of using the GISPP method that relies on ArcGIS (ESRI, 2011) Boundary Clean and Aggregate Polygons functions (Lines 143-148).

R3 – Minor Issue #1. L186 should be millions instead of thousands.

The reviewer is correct that this value could be millions but in some applications it is still thousands and so no edits were made.

R3 – Minor Issue #2. Citations for Streamflow Prediction Tool.

The Streamflow Prediction Tool (SPT) is used by the U.S. Army for streamflow predictions outside the Continental United States, while the National Water Model (NWM) is only for locations within the Continental United States. AutoRoute currently utilizes flow rates from the SPT but could also utilize flows from the NWM. Therefore, the citations to the SPT are relevant and no edits were made.

R3 – Minor Issue #3. Unclear as to what does "AutoRoute is operated in an ad-hoc basis" mean. Authors need to clarify this statement. Also, why only 70% of the world has SPT implementations?

Lines 40-44 were editd/included to better define the role of AutoRoute in an ad-hoc basis as well as state why SPT is operational for only ~70% of the world.

R3 – Minor Issue #4. A figure showing the geographic locations of these seven sites would be helpful to readers.

We agree with the reviewer and now included Figure 3 (also see Line 184), which shows the test site locations on a US map.

R3 - Minor Issue #4. Currently the authors only plainly presented statistics, but I suggest the authors discuss more about their difference. Is elevation the only difference that explain their different model performance?

Statistics were added to Section 4.1 and complexities due to terrain, land cover, topography, flow rates utilized, etc. are discussed as potential reasons for similarities and differences in model performance.

References

ESRI: ArcGIS Desktop: Release 10, Environmental Systems Research Institute, Redlands, CA, 2011.

GDAL/OGR Contributors: GDAL/OGR Geospatial Data Abstraction Software Library, Available from: https://gdal.org, 2019.

Improved Accuracy and Efficiency of Flood Inundation Mapping of Low-, Medium-, and High-Flow Events Using the AutoRoute Model

Michael L. Follum[1,2], Ricardo Vera[3], Ahmad A. Tavakoly[1,4], and Joseph L. Gutenson[1,5]

[1]Coastal and Hydraulics Laboratory, Engineer Research and Development Center, 3909 Halls Ferry Road, Vicksburg, MS 39180, USA
[2]Wyoming Area Office, U.S. Bureau of Reclamation, 705 Pendell Blvd., Mills, WY 82644, USA.
[3]Cold Regions Research and Engineering Laboratory, Engineer Research and Development Center, 72 Lyme Road, Hanover, NH 03755, USA
[4]Earth System Science Interdisciplinary Center, University of Maryland, College Park, MD 20740, USA
[5]National Water Center, National Oceanic and Atmospheric Administration, 205 Hackberry Ln, Tuscaloosa, AL 35401, USA

Correspondence to: Michael L. Follum (follumm@gmail.com)

Abstract. This article presents improvements and development of a post-processing module for the regional scale flood mapping tool, AutoRoute. The accuracy of this model to simulate low, medium, and high flow rate scenarios is demonstrated at seven test sites within the U.S. AutoRoute is one of the tools used to create high-resolution flood inundation maps at regional- to continental-scales~~. The model~~, but has previously only been tested using extreme flood events. ~~In this article~~Modifications to the AutoRoute model and post-processing scripts are shown to improve accuracy (e.g. average *F* value increase of 17.5% for low-flow events) and computational efficiency (simulation time reduced by over 40%) when compared to previous versions. Although flood inundation results for low-flow events are shown to be comparable with published values (average ~~F~~*F* value of 63.3~~%) but~~%), the model results tend to be overestimated, especially in flatter terrain. Higher-flow scenarios tend to be more accurately simulated (average F value of 77.5%). ~~Additionally, modifications to the AutoRoute model and post-processing scripts are shown to improve computational efficiency (i.e. simulation time) by over 40% when compared to previous versions.~~ With improved computational efficiency and the improved ability to simulate both low and high flow scenarios the AutoRoute model may be well suited to provide first-order estimates of flooding within an operational, regional- to continental-scale hydrologic modelling framework.

1 Introduction

Recent advances have demonstrated continental-scale flow forecasting models capable of simulating thousands of stream reaches simultaneously (e.g. National Water Model (NWM) (http://water.noaa.gov/about/nwm); Streamflow Prediction Tool (SPT) (Snow et al., 2016; Wahl 2016)). Although flow simulations at these scales are beneficial, water managers and emergency personnel benefit more from high-resolution flood inundation maps to make operational decisions (such as evacuation, road closures, etc.). Advanced hydraulic models typically operated from the reach-scale to the small-basin-scale have shown some success in simulating flood inundation at the continental scale (Wing et al., 2017), but at a high computational cost. Due to low data requirements, fast initial set-up times, and lower computational burden, lower-complexity hydraulic

models have been developed in recent years to simulate flood inundation quickly using continental-scale hydrologic modelling outputs. Although not meant to replace the higher-fidelity hydraulic models, these lower-complexity models can provide a reasonable first-order approximation of flood inundation over regional to continental extents and help prioritize where deployment of the higher-fidelity hydraulic models are needed (Follum et al., 2019). The National Oceanic and Atmospheric Administration (NOAA) National Water Center (NWC) has adopted the Height Above Nearest Drainage (HAND) model (Liu et al., 2018; Zheng et al., 2016) to use in conjunction with the NWM within the U.S. Due to a need for connecting hydrologic data to mobility models for the military, the U.S. Army Coastal and Hydraulics Laboratory (CHL) developed the AutoRoute flood and mobility model (Follum, 2012; Follum et al., 2017; McKinley et al., 2012). AutoRoute works in conjunction with the SPT (Follum et al., 2017) to provide hydrologic and mobility guidance in data sparse environments outside the continental United Stated (OCONUS). Currently SPT is run operationally (15-day streamflow forecasts updated twice daily) by CHL for approximately 70% of the world~~.~~ (between latitudes ~54°S and ~60°N based on data availability of the HydroSHEDS and HydroBASINS datasets (Lehner and Grill, 2013) from which SPT streamlines are derived). AutoRoute is currently operated in an ad-hoc basis when flood inundation or mobility assessments are required.

Both HAND and AutoRoute are raster-based models. Using the high-resolution National Hydrography Dataset Plus (NHDPlus) dataset (Horizon Systems Corporation, 2007; McKay et al., 2012) and a ~9 m digital elevation model (DEM), Liu et al. (2018) created HAND rasters for the entire U.S. A HAND raster simply shows the relative height of a cell above the nearest NHDPlus stream line (nearest in terms of drainage distance). Flow-depth rating curves are assigned to each stream reach (Zheng et al., 2018) so if given a flow rate the stage of the river can be calculated. Any HAND raster cell with a value less than the calculated river stage is considered flooded (inundated). However, this process relies heavily on pre-computed flow-depth relationships currently not available for much of the world.

AutoRoute was initially developed by CHL to automatically develop cross-sections along ephemeral streams/rivers to assess gap-crossing capabilities of military vehicles during flood events (Follum, 2012; McKinley et al., 2012). Because AutoRoute was utilized for ephemeral streams the channel profile (including bathymetry) was assumed to be represented by the DEM. Recently, AutoRoute has been applied with large-scale river routing models (such as the RAPID model (David et al., 2011; Tavakoly et al., 2017) within SPT) to simulate high-resolution (<30m spatial resolution) flood inundation maps over large extents: 230,000 km^2 area in the Midwest United States; 109,500 km^2 area in the Mississippi Delta (Follum et al., 2017); Sava River Basin; Puerto Rico (Follum et al., 2018); Navajo Nation (Follum et al., 2019); and Luzon, Philippines (Wahl et al., 2017). Stream networks (polyline format) within the U.S. are defined using the NHDPlus dataset. Outside the U.S. stream networks (polyline format) for approximately 70% of the world have been created using HydroSHEDS and HydroBASINS datasets (~~Lehner and Grill, 2013) (~~see Snow et al., 2015 for an example). AutoRoute converts the polyline stream locations to a raster or table format (see Follum et al. (2017) for details). Cross-sections are automatically sampled for each stream cell from a DEM and the normal depth is then calculated for a given flow rate using Manning's equation. The extent and depth of

flooding within the cross-section is then mapped to a raster format. Only cells within the raster used for cross-sections will show flood extent or depth. A post-processing step is often utilized where flood extent results in raster format are converted to a polygon format. The main purpose of the post-processing step is to overcome inaccuracies in the flood extents created by AutoRoute. Holes in the floodplain (cells not captured by cross-sections) are filled, the boundaries along the floodplain are smoothed, and outliers in the flood extent (cells that show flooding where no other surrounding cells show flooding) are omitted. Outliers in the flood map are caused by large variations in flow depths along a given stream reach (Afshari et al., 2018; Follum et al. 2017), often caused by high elevation values due to bridges (Follum et al. 2017) or spikes in the DEM; cross-sections not being sampled perpendicular to the stream channel; and errors in calculating the slope of the channel (related to errors in the stream network or DEM). It is expected that these variations in depth and flood extent will be more pronounced in low-flow events where differences in depth or inundation extent may be more evident in an inundation map. Computationally, the post-processing step takes almost as long as the execution of the AutoRoute model itself (Follum et al., 2017). Additionally, this post-processing step does not consider the terrain data; the post-processing is used only to make flood inundation maps appear more continuous.

Afshari et al. (2018) compared HAND, AutoRoute (with post-processing), and HEC-RAS 2D (USACE, 2016) at two locations: Cedar River watershed in Iowa, and the Black Warrior River in Alabama. Three statistical flow conditions were tested at each site, the 10-, 100-, and 500-yr flow rates. The HAND and AutoRoute models produced similar flood inundation maps when compared to the more-advanced HEC-RAS 2D model, but both HAND and AutoRoute showed less accuracy in meandering channels and near confluences. Overall, the AutoRoute model produced slightly higher flood extent accuracy than the HAND model. However, the AutoRoute model tended to have lower accuracy with lower flow events. This highlights a concern that the AutoRoute model has typically been tested for large flood events (flood events greater than the 50-yr flood were tested in Follum (2012), Follum et al. (2017; 2018; 2019), and Wahl et al. (2017)) and may not be applicable for less extreme flow events.

This article presents modifications to the AutoRoute model to better incorporate bathymetry estimations and terrain in the calculation and post-processing of flood inundation maps, which are expected to improve the flood mapping capability of the AutoRoute model for extreme (>50 yr flood event) and non-extreme flood cases. The modifications are expected to produce continuous and accurate flood extent results for both low and high flow events. The AutoRoute model is tested at seven locations within the U.S. where flood inundation maps for multiple flow rate scenarios (ranging from low to high flow events) have been modelled and compared to observed flow events by NOAA's Advanced Hydrologic Prediction Service (McEnery et al., 2005).

2 Methodology

2.1 AutoRoute Model

AutoRoute is a grid-based model where elevation, stream locations (stream cells), and land cover are defined using a raster format. Gridded stream cells were originally defined using a flow accumulation raster (Follum, 2012). With the creation of river networks in polyline format (e.g. NHDPlus and HydroSHEDS) stream cells are now created by converting polyline data to a raster or table format (table defines the x- and y- coordinates). Each stream cell retains the unique river reach identifier (e.g. ComID in NHDPlus) to associate attributes of the stream reach to each stream cell. For example, streamflow Q ($m^3\ s^{-1}$) from a hydrologic model, such as SPT or NWM, is assigned to each stream cell using the river reach identifier. At each stream cell, cross-sections are sampled from an elevation dataset (Figure 1). In the original AutoRoute model the channel profile is estimated only from the elevation dataset; no bathymetric profile is assumed. Although not assuming a bathymetric profile was acceptable in the original applications of AutoRoute where ephemeral streams were being simulated, AutoRoute is being used in more regions and inclusion of bathymetric profiles should improve flood inundation estimations (Dey et al., 2019) and mobility assessments. For each cross-section sampled AutoRoute now includes a bathymetry estimation. AutoRoute adjusts the centerline of the cross-section to the lowest point. The lateral distance that AutoRoute searches for the lowest point is specified by the user, typically defined as 20m. As shown in Figure 1, the cross-section sampled from the DEM often shows the stream/river as a flat surface. AutoRoute automatically finds the top-width (T, m) of the water surface and then estimates a bathymetric profile. The bathymetric profile is assumed to have an exponential shape, as shown in Figure 1. The exponential shape takes the form

$$y = \delta\,|x|^{\beta}, \quad (1)$$

where y (m) and x (m) are the ordinates of the bathymetric profile as shown in Figure 1 and δ is a user-defined parameter (assumed 0.001 for this paper). When x=0 the maximum depth of the bathymetric profile (Z, m) is assumed to occur ($y = 0$ based on the orientation of the y and x axes in Figure 1). When $x = T/2$ the bathymetric profile is at the bank of the river and $y = Z$. Based on these two constraints and Eq 1, β is calculated as

$$\beta = \frac{log(Z/\delta)}{log(T/2)}. \quad (2)$$

Using Manning's equation (described below), ~~the depth of the bathymetric profile is set~~Z is calculated so that a specified base flow will pass through the bathymetric profile. The bathymetric profile is burned into the cross-section profile and the centerline of the stream/river is again adjusted to the lowest point. Hydraulic area A (m^2) and wetted perimeter P (m) are calculated at each cross-section for a given flow depth D (m). Using a volume-fill approach D is incrementally increased until there is less than a 1% difference between Q and the calculated streamflow Q_{calc} ($m^3\ s^{-1}$), calculated using Manning's Equation:

$$Q_{calc} = \frac{c_u}{n} A^{5/3} P^{-2/3} S_f^{1/2}, \quad (~~1~~3)$$

where c_u is the unit constant (1.0 for metric units), n is the Manning's roughness coefficient, and S_f is the hydraulic slope. Normal depth is assumed, and therefore $S_f = S_o$, where S_o is the slope of the channel. AutoRoute calculates S_o by analyzing the elevations and lateral distances upstream and downstream of the stream cell being analyzed (more explanation found in Follum et al. (2017)). n is estimated as (Horton, 1933; Einstein, 1934):

$$n = \left[\sum_{i=1}^{N} \frac{P_i {n_i}^{1.5}}{P}\right]^{2/3}, \quad (24)$$

where P_i and n_i are wetted perimeter and Manning roughness coefficient of the ith segment within the cross-section, and N is the total number of segments within the cross-section that are flooded. n_i values are associated with land cover types, as described in Follum et al. (2017).

An initial cross-section is sampled perpendicular to the stream direction, as defined by positions of upstream and downstream stream cells. However, stream cross-sections may not always adequately capture the floodplain geometry, therefore multiple cross-sections are sampled for each stream cell by incrementally pivoting the cross-section relative to the stream direction. As shown in Follum et al. (2017), these multiple cross-sections have the effect of filling in the floodplain but can also create errant cross-sections and therefore errors in the floodplain mapping. The cross-section for each stream cell (subscript sc) that produces the shortest top width TW_{sc} (m) is expected to be the most representative cross-section for that stream cell. The TW_{sc} and the flow depth D_{sc} (m) of the representative cross-section are recorded for each stream cell.

AutoRoute originally created flood inundation and flood depth rasters by mapping all of the cross-section depths and extents onto a raster. ~~An~~ (Follum 2012). Later, an iterative combination of the Boundary Clean and Aggregate Polygons functions within ArcGIS (ESRI, 2011) was then used to fill-in holes, omit outlier flood cells, and smooth boundaries along the flood polygon. (Follum et al., 2017). None of the previous post-processing considered topography in the creation of the flood polygon. In this paper the use of Boundary Clean and Aggregate Polygons functions within ArcGIS (ESRI, 2011) are considered as the baseline method for post-processing AutoRoute results and is referred to as GIS Post-Processing (GISPP).

2.2 Development of AutoRoute post-processing script (ARPP)

The AutoRoute post-processing script (ARPP) has been developed to better account for topography when creating the flood inundation map. The water surface elevation of each stream cell WSE_{sc} (m) is calculated:

$$WSE_{sc} = E_c + D_{sc}, \quad (35)$$

where E_c (m) is the elevation of the cell. The water surface elevation for each cell in the model domain (WSE_c, m) is interpolated from the WSE_{sc} values using inverse-distance-weighting:

$$WSE_c = \frac{\sum WSE_{sc}\, w}{\sum w}, \quad (46)$$

where w is the weight, calculated as:

$$\begin{cases} w = {d_{c\to sc}}^{-2} & if \quad d_{c\to sc} \le \alpha\, TW_{sc} \\ w = 0 & if \quad d_{c\to sc} > \alpha\, TW_{sc} \end{cases} \quad (57)$$

where $d_{c\to sc}$ (m) is the distance between the model domain cell and the stream cell, and α is a user-defined parameter. Higher values of α increase the influence that each stream cell has on flooding the surrounding cells. The flood depth for each cell in the domain D_c (m) is then calculated as:

$$D_c = WSE_c - E_c, \quad (68)$$

where D_c values less than zero are set to zero and cells with D_c values greater than zero are considered flooded. All flooded cells are then converted to a polygon format.

Figure 2 (top) demonstrates the flooding (D_c values) of the surrounding terrain from a single stream cell. When the depths from all stream cells are included by use of Eqs. 46 and 57 the flooding of the surrounding cells provides a continuous flood map with holes only in the high-elevation areas (bottom frame of Figure 2). Additionally, stream cells that have WSE_{sc} values higher/lower than surrounding stream cells (i.e. outliers) have impact only on the immediately surrounding cells (see shallow locations within river in bottom frame of Figure 2). These outliers can be caused by cross-sections not being perpendicular to the stream reach, errors in hydraulic slope estimation, and errors within the DEM. Although these outliers affect the immediately surrounding cells, they have minimal impact on flooding in the floodplain. However, these outliers could affect channel profiles for mobility analysis and should be addressed in future research. The minimal impact of outliers on flood inundation is due to the influence of water surface elevations from multiple stream cells on each WSE_c value. Use of ARPP to post-process AutoRoute flood depth results is expected to produce more continuous flood maps, account for topography, and reduce the impact of errant D_{sc} values on the flood inundation results, all of which are expected to be important in simulating both low- and high-flow events.

2.3 Study Locations

For several communities throughout the United States the USGS has created flood inundation maps for multiple water surface elevations (stages) of the river. These maps are intended to be used in conjunction with National Weather Service (NWS) forecasted peak-stage data to show predicted areas of flooding. The modelled stage heights vary between the sites, but are intended to capture the river stage at multiple (often around 20) stages between normal conditions (low flow) and the highest rated stage at the streamgage (high flow). The hydraulic model used to create the flood inundation maps varies between the sites, but each model is validated against observed flood events. For this study seven locations where the U.S. Geological Survey (USGS) has completed flood inundation studies were chosen. (Figure 3). Each site varies in complexity as well as geographical location (multiple river basins throughout the U.S.).

For each site used in this study Table 1 lists the location, identification (ID), river(s), USGS streamgage number, length of river segments within the study, and reference. All studies utilized LiDAR elevation datasets ranging between 0.9 and 3 m

horizontal spatial resolution. Each study also used the HEC-RAS hydraulic model (USACE, 2010; 2016). Each study calibrated and validated the hydraulic models to observed flood data.

Table 2 lists the base flow and the low, medium, and high flow rates used in the study. The low, medium, and high flow rates were chosen based on the minimum, median, and maximum modelled flow rates in each of the USGS studies (a flow rate was assigned to each stage height in each of the studies). The USGS does not provide base flow estimates for the sites in this study, so the base flow was estimated as the average annual flow rate for each gage listed in Table 1. The annual flow rates were obtained from USGS WaterWatch (https://waterwatch.usgs.gov/?id=ww_current; visited 01 Feb 2019). USGS streamgage 02126375 along the Pee Dee River (Figure ~~6~~8) does not record flow rates, so the flow data from the USGS streamgage 0212378405 approximately 12-km upstream along the Pee Dee River was used to estimate baseflow. Brown Creek and Rocky River are also included in the NC study (Smith and Wagner, 2016), but are omitted from this study because flow rates were unavailable. The USGS streamgage 02473000 along the Leaf River is used in the MS study and is less than 1 km downstream of the confluence of the Leaf and Bouie Rivers (Figure ~~7~~9). Above the confluence of the rivers the Leaf and Bouie Rivers are assumed to carry approximately 70% and 30%, respectively, of the flow rates measured at the USGS streamgage 02473000 (Storm, 2014).

3 Model Application

AutoRoute models were developed for each of the seven test locations. Each model was developed using elevation data from the 1/3-arc-second (~9 m) National Elevation Dataset (Gesch et al., 2002), and land cover classifications were obtained from the 2011 National Land Cover Database (NLCD) (Homer et al., 2015). The NLCD has a spatial resolution of approximately 30 m and therefore was resampled to the resolution of the DEM. The stream networks for each study site were defined using the NHDPlus dataset.

~~The AutoRoute model has few calibration parameters. Following Follum et al. (2017), n_s values were set to the lower bound as described in Moore (2011), Chow (1959), and Calenda et al. (2005). The number of cross-sections sampled at each stream cell was set to 9 following Follum et al. (2017). The influence that each stream cell has on flooding the surrounding cells is controlled by the user-defined α parameter. When tested, setting α to 1.5 provided good coverage of the river floodplain while remaining computationally efficient.~~

For each simulation, the qualitative performance of the AutoRoute models compared to the USGS data are measured using the F-statistic (F, percentage) (Bates and De Roo, 2000; Tayefi et al., 2007) and error bias (E) (Wing et al. 2017):

$$F = 100\left(\frac{A_{Acc}}{A_{Obs}+A_{Sim}-A_{Acc}}\right), \quad (~~7~~9)$$

$$E = \frac{A_{Over}}{A_{Under}}, \quad (~~8~~10)$$

where A_{Obs} (km^2) is the area of flooding from the USGS flood maps, A_{Sim} (km^2) is the area of flooding from the AutoRoute simulation, A_{Acc} (km^2) is the area where both AutoRoute and the USGS show flooding, A_{Over} (km^2) is the area where only the AutoRoute model shows flooding, and A_{Under} (km^2) is the area where only the USGS flood maps shows flooding. F ranges between 0 and 100% with a value of 100% indicating perfect fit between the AutoRoute and USGS flood inundation maps. Previous applications of AutoRoute within the U.S. have had F values between 58.4 and 92.5% (Follum et al., 2017), with the IN test site having an F value of 77% when compared to observed flood maps from the June 2008 flood. E ranges between 0 and ∞ with E values less than 1indicating a bias towards underestimation, E values greater than 1indicating a bias towards overestimation, and an E value of 1 indicating no bias.

The AutoRoute model has few calibration parameters. Following Follum et al. (2017), n_i values were set to the lower bound as described in Moore (2011), Chow (1959), and Calenda et al. (2005). The number of cross-sections sampled at each stream cell was set to 9 following Follum et al. (2017). The influence that each stream cell has on flooding the surrounding cells is controlled by the user-defined α parameter. A sensitivity analysis was performed to determine the affect α has on the flood inundation when using ARPP post-processing. Using all seven test sites and all three flow scenarios α was varied between 0.25 and 3.0 by increments of 0.25. Figure 4 shows the F value associated with each of the 252 simulations. Increases in α tend to result in an increase in accuracy (higher F values). However, increases in α also increase the computational burden. For example, four times as many cells are analysed for each stream cell when α=3.0 than when α=1.5. For this study α is set to 1.5 because it provides good coverage of the river floodplain (and thus higher F values) while remaining computationally efficient.

4 Results and Discussion

4.1 Flood Inundation Mapping

For each study site the low, medium, and high flow scenarios were simulated using AutoRoute. The results were then post-processed using the ARPP method (AutoRoute+ARPP) described in this paper as well as the original GISPP method (AutoRoute+GISPP). The only difference between AutoRoute+GISPP and AutoRoute+ARPP results is the post-processing method used. For each test case Table 3 shows the quantitative performance (F and E) of flood inundation maps simulated using AutoRoute+ARPP and AutoRoute+GISPP as compared to the USGS flood inundation maps. Table 3 also shows the value of A_{Obs}, A_{Sim}, A_{Over}, A_{Under}, and A_{Acc} ~~with the results being post-processed using the ARPP. Figures 3-5 show a comparison between the flood inundation maps generated by AutoRoute and the USGS flood maps.~~ for each flood inundation map simulated using AutoRoute+ARPP. Overall, the use of ARPP results in improved flood inundation accuracy when compared to GISPP (average F value is 7.4% higher when using ARPP). The increase in accuracy of the ARPP method is most evident in the low-flow scenarios where the average F value increases from 45.8% when using GISPP to 63.3% when

using ARPP. For the med-flow scenarios the average F value increases from 65.7% when using GISPP to 70.0% when using ARPP. The difference in F value for the high-flow scenario is minimal when using GISPP (77.2%) and ARPP (77.5%). Flooding results are split between overestimation (E>1) and underestimation (E<1) when using the ARPP method (10 test cases underestimated and 11 test cases overestimated), while the GISPP method is more prone to overestimation (6 test cases underestimated and 15 test cases overestimated). Overall, the use of ARPP improved the accuracy (higher F value) of the flood results in 18 of the 21 test cases.

Figures 5-7 show a comparison between flood inundation maps generated using AutoRoute+ARPP and the USGS flood maps. In the figures the areas shaded green (Accurate) indicate areas where AutoRoute+ARPP and the USGS flood maps agree. Areas shaded red (Over) indicate where only AutoRoute+ARPP simulates the area as flooded and areas shaded blue (Under) indicate where only the USGS shows the area as flooded. ~~For each test case Table 3 shows~~ The accuracy of the ~~value of A_{obs}, A_{sim}, A_{Over}, A_{Under}, and A_{Acc}, as well as the quantitative performance (F and E) of flood inundation maps simulated using AutoRoute compared to the USGS flood inundation maps.~~

~~The~~ flood maps generated using low flows ~~have an (~~average F value of 63.3~~%, which%)~~ are comparable with results from other studies (Afshari et al., 2017; Dey et al., 2019; Follum et al., 2017; Tayefi et al., 2007), but tend to overestimate flooding (all E values are greater than 1 except for the CO test site). Although IN has the highest E value, the high F value and Figure ~~3~~5 show the flood map during the low flow event is accurately simulated and the E value is inflated due to the minimal underestimation of flooding (Table 3). Visually and quantitatively, NC and MS (Figure ~~3~~5 and Table 3) have the greatest amount of overestimation during the low flow event, resulting in the lowest F values of all the simulations. NC shows overestimation in low-lying areas adjacent to the river where the ARPP allows for flooding in areas even if they are not hydraulically connected to the streamlines, resulting in the lowest overall F value of 39.3%. MS also shows gross overestimation of flooding during the low-flow event. MS has minimal topography, a characteristic that has shown AutoRoute to produce less accurate results (Follum et al., 2017). AutoRoute simulations are essentially one-dimensional (1D); better representation of hydrodynamics in areas with minimal topography occurs with multi-dimensional modelling. Additionally, MS has the highest ratio of low flow to base flow (the low flow used in this study is over 15 times the flow rate of the base flow) which may have led to errors in bathymetry estimation if the elevation dataset was derived during a higher flow event. The coarse resolution used in this study compared to the USGS study may also contribute to inaccuracies (e.g. overestimation) that may be more pronounced in flatter terrain such as MS. While most streams considered in this analysis lie in rural land use environments, such as forested or agricultural areas, MS occurs in a primarily urban to sub-urban environment where small-scale changes in the topography are smoothed or negated in the relatively coarse ~9 m DEM. Many of these missed topographic features are likely flood control structures, such as levees. The combination of minimal topography, DEM inaccuracies, and land use complexities likely led to the overestimation found in the MS study.

With a few exceptions (e.g. SC), the flood maps generated for the med-flow events (*F* value of 70.0%; Figure 6) and high-flow events (*F* value of 77.5%; Figures ~~4 and 5~~7) are more accurate than the flood maps generated for the low-flow events (~~Figure (~~*F* value of 63.3%; Figure 5). This finding is consistent with flood mapping results using the HEC-RAS hydraulic model in recently published work (Dey et al., 2019). They also showed that the median of F values is higher with increasing flow. ~~The average *F* value for med-flow events is 70.0% and average *F* value for high-flow events is 77.5%.~~ The maximum *F* value of 92.6% occurs at NC during the med flow (NC had the lowest overall *F* value during the low-flow event). The sudden increase in *F* value between the flood maps generated using low-flow and med-flow at NC is due to the low-lying terrain near the river being simulated as flooded by both AutoRoute+ARPP and the USGS during the med-flow event, thus reducing the overestimation and increasing the accuracy. Although flood maps for the med- and high-flow events tend to have higher *F* values, they also tend to have a bias to underestimate the flooded area (*E* values less than 1). The majority of underestimation at the IN test site (Figures ~~4~~6 and ~~5~~7) occurs where a tributary (Meadowbrook Creek) that is not accounted for in the AutoRoute simulation flows into the White River to the south and west of the town of Spencer.

The two test locations along the Deerfield River in Massachusetts (MC and MW) show consistent accuracy between the low-, med-, and high-flow rates. This region of Massachusetts has well-defined rivers and medium to high topographic relief. These features allow AutoRoute to better capture the riverbanks and floodplain, resulting in consistent accuracy (*F* values close to 100) and minimal bias (*E* values close to 1).

4.2 Flood Inundation Mapping Test Using High-Resolution DEM

~~A~~Elevation datasets are used in flood mapping to define the topographic features (slopes, banks, levees, etc.) of the area being modelled, therefore the spatial resolution and vertical accuracy of the elevation datasets being used have a large impact on the accuracy of flood inundation maps being generated (Ali, Solomatine, and Di Baldassarre, 2015; Brandt and Lim, 2012; Cook and Merwade, 2009; Hsu et al., 2016). A thorough investigation of the impacts of various elevation datasets on the accuracy of flood inundation maps generated using AutoRoute+ARPP is outside the scope of this paper. However, a simple test is employed to determine if a high-resolution DEM (~3 m) improves the flood inundation accuracy when using AutoRoute ~~and~~ +ARPP. The MS and NC sites had the most overestimation of flooding during the low flow event when using a ~9 m resolution DEM and are therefore used in this test. A 1/9-arc-second (~3 m) National Elevation Dataset (Gesch et al., 2002) elevation dataset replaces the ~9 m elevation dataset. The NLCD was resampled to 1/9 arc-second, but all other data remains the same from the previous tests. Figures ~~6~~8 and ~~7~~9 show the high-resolution flood inundation for low-, med-, and high-flow events at NC (NC-3m) and MS (MS-3m), respectively. Table 3 shows the quantitative performance for flood inundation maps simulated using AutoRoute+ARPP compared to the USGS flood inundation maps. Table 3 and Figures ~~3-6~~5-8 show the flood results for NC and NC-3m are similar for each of the flow events. Even with the high-resolution DEM the model still simulates flooding in the low-lying terrain near the river in the low-flow event (Figures ~~3~~5 and ~~6~~8), thus resulting in a high overestimation (high *E* and A_{over} values in Table 3). Comparing the simulated area (A_{sim}) for the MS test site the model using 3-m DEM

data produced a flood map having approximately half the area of the flood map using a ~9 m DEM (Figures ~~3~~5 and ~~7~~9). For the med- and high-flow test cases the A_{Sim} values were approximately 78% and 97%, respectively, of the values when using a ~9 m DEM. Use of higher resolution at the MS test site produced smaller A_{Sim} values (Table 3 and Figure ~~7~~9), especially for smaller flood events. Although smaller A_{Sim} values resulted in lower A_{Over} values for MS-3m, they also resulted in higher A_{Under} values which showed a bias of the model to underestimate the flooded area and therefore the F values did not improve when compared to the MS results. In general, the higher resolution DEM did not substantially improve flood inundation results in NC or MS as expected.

Regardless of DEM resolution, inaccuracies in flood inundation results may be due to the use of constant n_i values that are set solely based on land cover maps. Not only are roughness coefficients likely different even under the same land cover types, but the values of n_i also vary with the depth of water (Ree and Palmer, 1949; Temple et al., 1987). In this study the low estimate of n_i values were used based on Follum et al. (2017). However, that study did not include bathymetry estimation within the cross-sections and therefore a reexamination of the proper of n_i values to use within AutoRoute may be warranted. Another source of error may be the simple bathymetry estimation for each cross-section. A more detailed bathymetry would affect the low-flow scenario the most but would likely improve the accuracy of flood inundation for all flow scenarios.

4.3 Simulation Time

On average, each flow event for each test case using the ~9 m DEM took approximately 12 seconds to read all data (elevation, land cover, stream location, and flow rates) into memory, simulate flood depth results using AutoRoute, post-process the flood depth results into raster flood maps using ARPP, and convert the raster flood maps into flood inundation polygons. For the high-resolution test locations (MS-3m and NC-3m) each test case took over 90 seconds. However, all of the test cases were for relatively small areas whereas the main reason to utilize a simplified hydraulics model such as AutoRoute is for computational efficiency when simulating flood inundation along thousands of river reaches at the regional- to continental-scale. Therefore, to compare computation times to the original AutoRoute methods described in Follum et al. (2017) the same domains in the Midwest (230,000 km^2 area) and Mississippi Delta (109,500 km^2 area) were simulated again using the methods described in this paper~~.~~ (AutoRoute+ARPP). Similar to Follum et al. (2017), the domains were discretized into thirty-nine 1° by 1° tiles (as defined by how USGS NED data is disseminated). Flow rates from Tavakoly et al. (2017) were once again used to define the peak flow in each river reach in the domain. The AutoRoute simulations in Follum et al. (2017) required approximately 20-minutes to simulate a 1° by 1° tile, compared to 17.5-minutes using the current version of AutoRoute. The current version of AutoRoute is more computationally efficient through the use of the Geospatial Data Abstraction Library (GDAL/OGR Contributors, 2019) for reading and writing data. The post-processing procedure (i.e. GISPP) described in Follum et al. (2017) required approximately 15-minutes for each 1° by 1° tile. Post-processing using ARPP to convert flood depth data to a flood depth raster and flood polygon takes approximately 3 minutes. Overall, the current version of AutoRoute and the use of ARPP is over 40% more computationally efficient in simulating flood inundation maps.

The increased computational efficiency of AutoRoute and ARPP along with removing the requirement for ArcGIS software in post-processing may allow for the AutoRoute model to more effectively be implemented on computational servers by CHL to provide flood and mobility assessments for OCONUS applications. These assessments will likely use SPT for streamflow data and be operated at the regional-scale using a 1° by 1° spatial discretization. A further modification to improve computational efficiency may be to create a database of AutoRoute simulations for varying flow rates. When forecast flowrates become available the database could be used instead of an AutoRoute simulation to determine the depth within each stream cell. ARPP could then be used to generate the flood maps. This type of database could also provide flow-depth relationships to be used with the HAND method. Additionally, a production system could determine if streams within each modelling domain cross a specified bankfull streamflow threshold and AutoRoute simulations would only occur if the streamflows for a given hydrometeorlogical forecast exceeded these bankfull thresholds. Either process may further improve the computational efficiency in creating production flood inundation maps.

5 Conclusions

The AutoRoute model is a simplified hydraulics model designed to quickly provide high-resolution flood inundation and mobility results at the regional to continental scale. The main purpose of this paper was to test the computational efficiency and accuracy of flood inundation maps generated by the AutoRoute model with special consideration given to less-extreme flow events (i.e. low and medium flood events). Seven test ~~cases~~sites were chosen to compare flood ~~inundantion~~inundation maps using low-, medium-, and high-flow rates. The seven test sites used a ~9 m elevation dataset and the locations correspond to existing USGS flood inundation studies and represent different regions within the U.S. The primary conclusions of the paper are as follows:

~~1.)~~ Implementation of a new post-processing procedure improved the flood inundation accuracy of the AutoRoute model, especially when simulating low-flow events (average *F* value increase of 17.5% when compared to previous post-processing methods). ~~Recent updates to the input and output methods within AutoRoute model as well as the post-processing procedure allow for the creation of flood inundation rasters (~9 m resolution) and polygons in 20.5 minutes for a 1° by 1° area, as compared to 35 minutes in previous studies. Increased computational efficiency may allow for the AutoRoute model to more effectively be implemented in a production environment at the regional to continental scale.~~

~~2.)~~1.) Although the flood inundation results for low-flow events are comparable with other studies (average *F* value of 63.3%), the simulated flooding tends to be overestimated. Higher-flow scenarios tend to be more accurately simulated (*F* value for medium-flow events is 70.0% and average *F* value for high-flow events is 77.5%). Simplifications in estimating roughness coefficients, cross-section profiles (including bathymetry

estimation), and the hydraulic simulation allow for AutoRoute to be computationally efficient but also may lead to errors in flood map simulation.

2.) Recent updates to the input and output methods within AutoRoute model as well as the post-processing procedure allow for the creation of flood inundation rasters (~9 m resolution) and polygons in 20.5 minutes for a 1° by 1° area, as compared to 35-minutes in previous studies. Increased computational efficiency may allow for the AutoRoute model to more effectively be implemented in a production environment at the regional to continental scale.

3.) Use of higher-resolution (~3 m) elevation data within the AutoRoute model was also tested at two of the sites and did not significantly improve the accuracy of the flood inundation maps. One of the sites showed only minimal difference in flood inundation when using the higher-resolution elevation data. The second site had an almost 50% reduction in simulated area for the low-flow test case, which reduced the overestimation of flooded area but also increased the underestimation of flooded area. Use of the higher-resolution elevation datasets increased computation time by 750% compared to when the ~9 m elevation dataset was used.

4.) As has been found in other studies, AutoRoute performs best in areas with mid-to-high topographic relief where one-dimensional flood models often perform well. Areas of minimal relief are more susceptible to back-water effects. AutoRoute physics do not account for such physical complexities and model results tend to be less accurate. As such, flood inundation results from AutoRoute should be viewed as a first-order approximation with the use of more detailed hydraulic models providing more actionable flood data.

The scope of this research was limited to small and medium inland rivers within the U.S. Several areas of future research were highlighted, including the need to better estimate roughness coefficients based on land cover and to account for change in roughness with flow depth. Improved elevation data and bathymetry estimation could improve both the flood inundation estimates and mobility assessment when using AutoRoute. Based on the recent work by Dey et al. (2019), different bathymetric methods could be implemented into AutoRoute for differing geomorphological conditions. Removal of outlier flood depth values will also improve the flood inundation estimation as well as the channel profiles that are used for mobility analysis. Use of a database system to store precomputed AutoRoute results could also improve efficiency and connect to other hydraulic models, such as HAND. Flood inundation models capable of quickly providing high-resolution flood maps have seen great improvement over the past decade as regional- to continental-scale flow simulation models are becoming operationalized by the U.S. Army, NOAA, and others. While the flow and flood inundation models continue to improve, the connection between the flood maps generated and the impacts to the population/environment need to become more fully-developed.

Acknowledgements

This project was supported by the Deputy Assistant Secretary of the Army for Research and Technology through the Engineer Research and Development Center's Military Engineering applied research work package title Austere Entry; the Geospatial Intelligence Directorate of the Marine Corps Intelligence Activity; and ERDC's collaborative research project supporting the NOAA National Water Center. We would also like to acknowledge the anonymous reviewers for their insightful comments that helped improve this article.

References

Afshari, S., Tavakoly, A. A., Rajib, M. A., Zheng, X., Follum, M. L., Omranian, E. and Fekete, B. M.: Comparison of new generation low-complexity flood inundation mapping tools with a hydrodynamic model, J. Hydrol., 556, 539–556, doi:10.1016/j.jhydrol.2017.11.036, 2018.

Ali, A.M., Solomatine, D.P., Di Baldassarre, G., Assessing the impact of different sources of topographic data on 1-D hydraulic modelling of floods, Hydrology and Earth System Sciences, 19(1), 631–643. doi: 10.5194/hess-19-631-2015, 2015.

Bates, P. D. and De Roo, A. P. J.: A simple raster-based model for flood inundation simulation, J. Hydrol., 236(1–2), 54–77, doi:10.1016/S0022-1694(00)00278-X, 2000.

Benedict, S. T., Caldwell, A. W. and Clark, J. M.: Flood-inundation maps for the Saluda River from Old Easley Bridge Road to Saluda Lake Dam near Greenville, South Carolina., U.S. Geological Survey Scientific Investigations Map 3244, 2013.

Brandt, S.A. and Lim, N.J., Importance of river bank and floodplain slopes on the accuracy of flood inundation mapping, In: R.E. Murillo Muñoz (Ed.), River Flow 2012: Volume 2. Proceedings of the International Conference on Fluvial Hydraulics, San José, Costa Rica, 5-7 September 2012, 1015-1020, Leiden, The Netherlands: CRC Press/Balkema (Taylor & Francis), 2012.

Calenda, G., Mancini, C. P. and Volpi, E.: Distribution of the extreme peak floods of the Tiber River from the XV century, Adv. Water Resour., 28(6), 615–625, doi:10.1016/j.advwatres.2004.09.010, 2005.

Chow, V. T.: Open Channel Hydraulics, McGraw-Hill Book Company Inc, New York City, New York, 1959.

Cook, A., Merwade, V.: Effect of topographic data, geometric configuration and modeling approach on flood inundation mapping, Journal of Hydrology, 377(1-2): 131-142, doi:10.1016/j.jhydrol.2009.08.015, 2009.

David, C. H., Maidment, D. R., Niu, G.-Y., Yang, Z.-L., Habets, F. and Eijkhout, V.: River Network Routing on the NHDPlus Dataset, J. Hydrometeorol., 12(5), 913–934, doi:10.1175/2011JHM1345.1, 2011.

Dey, S., Saksena, S., Merwade, V.: Assessing the Effect of Different Bathymetric Models on Hydraulic Simulation of Rivers in Data Sparse Regions, Journal of Hydrology, 575, 838-851, 2019.

Einstein, H. A.: The Hydraulic Cross Section Radius, Schweizerische Bauzeitung, 103(8), 89–91, 1934.

ESRI: ArcGIS Desktop: Release 10, Environmental Systems Research Institute, Redlands, CA, 2011.

Follum, M. L.: AutoRoute Rapid Flood Inundation Model, Coastal and Hydraulics Engineering Technical Note ERDC/CHL CHETN-IV-88. U.S. Army Engineer Research and Development Center, Coastal and Hydraulics Laboratory, Vicksburg, Mississippi 2012.

Follum, M. L., Gutenson, J. L., Wahl, M. D., Hunter, C. J. and Maldonado Linas, J. E.: Rapid Flood Inundation Modeling, Mil. Eng., 110(715), 37–38, 2018.

Follum, M. L., Paredez, J. M., Yeates, E. M. and Vera, R.: Utilizing Simple Large-Scale Flood Models to Prioritize Deployment of HEC-RAS 2D Models: Case Study of Navajo Nation Flood Inundation Maps, Flood Risk Management Newsletter , 12(2), 4–7, 2019.

Follum, M. L., Tavakoly, A. A., Niemann, J. D. and Snow, A. D.: AutoRAPID: A Model for Prompt Streamflow Estimation and Flood Inundation Mapping over Regional to Continental Extents, J. Am. Water Resour. Assoc., 53(2), 280–299, doi:10.1111/1752-1688.12476, 2017.

GDAL/OGR Contributors: GDAL/OGR Geospatial Data Abstraction Software Library, Available from: https://gdal.org, 2019.

Gesch, D. B., Oimoen, M., Greenlee, S., Nelson, C., Steuck, M., and Tyler, D: The National Elevation Dataset, Photogrammetric Engineering and Remote Sensing, 68(1):5-32, DOI: 10.1007/978-94-007-6769-0_1, 2002.

Homer, C., Dewitz, J., Yang, L., Jin, S., Danielson, P., Xian, G., Coulston, J., Herold, N., Wickham, J. and Megown, K.: Completion of the 2011 National Land Cover Database for the Conterminous United States – Representing a Decade

of Land Cover Change Information, Photogramm. Eng. Remote Sensing, 81(5), 345–354, doi:10.14358/PERS.81.5.345, 2015.

Horizon Systems Corporation: National Hydrography Dataset Plus: Documentation, Available from: http://www.horizon-systems.com/NHDPlus/NHDPlusV1_home.php, 2007.

Horton, R. E.: Separate Roughness Coefficients for Channel Bottom and Sides, Eng. News Rec., 111(22), 652–653, 1933.

Hsu, Y-C., Prinsen, G., Bouaziz, L., Lin, Y-J., Dahm, R., An Investigation of DEM Resolution Influence on Flood Inundation Simulation, Procedia Engineering, (154), 826-834, doi: 10.1016/j.proeng.2016.07.435, 2016.

Kohn, M. S. and Patton, T. T.: Flood-inundation maps for the South Platte River at Fort Morgan, Colorado, U.S. Geological Survey Scientific Investigations Report 2018–5114, Available from: https://doi.org/10.3133/sir20185114, 2018.

Lehner, B. and Grill, G.: Global river hydrography and network routing: Baseline data and new approaches to study the world's large river systems, Hydrol. Process., 27(15), 2171–2186, doi:10.1002/hyp.9740, 2013.

Liu, Y. Y., Maidment, D. R., Tarboton, D. G., Zheng, X. and Wang, S.: A CyberGIS Integration and Computation Framework for High-Resolution Continental-Scale Flood Inundation Mapping, J. Am. Water Resour. Assoc., 54(4), 770–784, doi:10.1111/1752-1688.12660, 2018.

Lombard, P. J. and Bent, G. C.: Flood-inundation maps for the Deerfield River, Franklin County, Massachusetts, from the confluence with the Cold River tributary to the Connecticut River, U.S. Geological Survey Scientific Investigations Report 2015–5104, Available from: http://dx.doi.org/10.3133/sir20155104, 2015.

McEnery, J., Ingram, J., Duan, Q., Adams, T. and Anderson, L.: NOAA's Advanced Hydrologic Prediction Service, Bull. Am. Meteorol. Soc., 86(3), 375–386, doi:10.1175/BAMS-86-3-375, 2005.

McKay, L., Bondelid, T., Rea, A., Johnston, C., Moore, R. and Deward, T.: NHDPlus Version 2: User Guide., 2012.

McKinley, G. B., Mason, G. L., Follum, M. L., Jourdan, M. R., LaHatte, C. W. and Ellis, J.: A Route Corridor Flood Vulnerability System, Geotechnical and Structures Laboratory Technical Report ERDC/GSL TR-12-29. U.S. Army Engineer Research and Development Center, Geotechnical and Structures Laboratory, Vicksburg, Mississippi, 2012.

Moore, M. R.: Development of a High-Resolution 1D/2D Coupled Flood Simulation of Charles City, Iowa, M.S. Thesis, University of Iowa., 2011.

Nystrom, E. A.: Flood-inundation maps for the White River at Spencer, Indiana, U.S. Geological Survey Scientific Investigations Map 3251, Available from: http://pubs.usgs/gov/sim/3251/, 2013.

Ree, W. and Palmer, V.: Flow of water in channels protected by vegetative linings, U.S. Dept. of Agriculture, No. 967, 1949.

Smith, D. G. and Wagner, C. R.: Hydraulic model and flood-inundation maps developed for the Pee Dee National Wildlife Refuge, North Carolina, U.S. Geological Survey Scientific Investigations Report 2015–5137, Available from: http://dx.doi.org/10.3133/sir20155137, 2016.

Snow, A. D.: A New Global Forecasting Model to Produce High-Resolution Stream Forecasts, MS Thesis, Brigham Young University - Provo., 2015.

Snow, A. D., Christensen, S. D., Swain, N. R., Nelson, E. J., Ames, D. P., Jones, N. L., Ding, D., Noman, N. S., David, C. H., Pappenberger, F. and Zsoter, E.: A High-Resolution National-Scale Hydrologic Forecast System from a Global Ensemble Land Surface Model, J. Am. Water Resour. Assoc., 52(4), 950–964, doi:10.1111/1752-1688.12434, 2016.

Storm, J. B.: An expanded model—Flood-inundation maps for the Leaf River at Hattiesburg, Mississippi, U.S. Geological Survey Scientific Investigations Map 3300, Available from: http://dx.doi.org/10.3133/sim3228, 2014.

Tavakoly, A. A., Snow, A. D., David, C. H., Follum, M. L., Maidment, D. R. and Yang, Z. L.: Continental-Scale River Flow Modeling of the Mississippi River Basin Using High-Resolution NHDPlus Dataset, J. Am. Water Resour. Assoc., 53(2), 258–279, doi:10.1111/1752-1688.12456, 2017.

Tayefi, V., Lane, S. N., Hardy, R. J. and Yu, D.: A comparison of one- and two-dimensional approaches to modelling flood inundation over complex upland floodplains, Hydrol. Process., 21, 3190–3202, doi:10.1002/hyp.6523, 2007.

Temple, D. M., Robinson, K. M., Ahring, R. M. and Davis, A. G.: Stability Design of Grass- lined Open Channels, Agric. Handb., 667, 1987.

U.S. Army Corps of Engineers: HEC-RAS River Analysis System, hydraulic reference manual, 2010.

U.S. Army Corps of Engineers: HEC–RAS River Analysis System, hydraulic reference manual, 2016.

Wahl, M. D., Follum, M. L., Snow, A. D. and Tavakoly, A. A.: Developing Hydrologic Awareness, Mil. Eng., 108(700), 2016.

Wing, O. E. J., Bates, P. D., Sampson, C. C., Smith, A. M., Johnson, K. A. and Erickson, T. A.: Validation of a 30 m resolution flood hazard model of the conterminous United States, Water Resour. Res., 53(9), 7968–7986, doi:10.1002/2017WR020917, 2017.

Zheng, X., Maidment, D. R., Tarboton, D. G., Liu, Y. Y. and Passalacqua, P.: GeoFlood: Large-Scale Flood Inundation Mapping Based on High-Resolution Terrain Analysis, Water Resour. Res., 54(12), 10,013-10,033, doi:10.1029/2018WR023457, 2018.

Zheng, X., Maidment, D., Liu, Y., Tarboton, D. G. and Lin, P.: From Forecast Hydrology to Real-Time Inundation Mapping at Continental Scale, in AGU Fall Meeting, Available from: https://agu.confex.com/agu/fm16/meetingapp.cgi/Paper/186012, 2016.

Tables and Figures

Table 1: USGS study sites used in this study. For each study site the location, ID, river(s), USGS streamgage, model length, and reference are provided.

Location	ID	River(s)	USGS Streamgage Number	Model Length (km)	Reference
Spencer, IN	IN	White River	03357000	8.5	Nystrom (2013)
Fort Morgan, CO	CO	S. Platte River	06759500	7.2	Kohn and Patton (2018)
Greenville, SC	SC	Saluda	02162500	6.4	Benedict et al. (2013)
Pee Dee, NC	NC	Pee Dee River	02126375	17.0	Smith and Wagner (2016)
Hattiesburg, MS	MS	Leaf and Bouie Rivers	02473000	10.9	Storm (2014)
Charlemont, MA	MC	Deerfield River	01168500	14.6	Lombard and Bent (2015)
West Deerfield, MA	MW	Deerfield River	01170000	14.3	Lombard and Bent (2015)

Table 2: Base flow and Low, Medium (Med), and High flow rates for each study site.

ID	Base Flow ($m^3 s^{-1}$)	Low Flow ($m^3 s^{-1}$)	Med Flow ($m^3 s^{-1}$)	High Flow ($m^3 s^{-1}$)
IN	83.9	164.0	577.7	2027.5
CO	16.6	79.9	577.7	2814.7
SC	17.2	79.6	222.9	373.8
NC	145.4	911.8	3021.1	7391.8
MS	63.5	999.6	1730.2	3409.3
MC	25.9	311.5	996.8	2415.4
MW	38.2	455.9	1659.4	3344.2

Table 3: F-statistic (*F*, percentage~~),~~) and error bias (*E*~~), and inundation~~) for AutoRoute+ARPP and AutoRoute+GISPP for each flow scenario at all seven test location. Inundation coverage areas (A_{Obs}, A_{Sim}, A_{Over}, A_{Under}, and A_{Acc}) are also shown for ~~each flow scenario at all seven test locations.~~AutoRoute+ARPP. *F* ranges between 0 and 100% with a value of 100% indicating perfect fit between the ~~AutoRoute~~simulated and USGS flood inundation maps. *E* values less than 1indicate a bias towards underestimation, *E* values greater than 1 indicate a bias towards overestimation, and an *E* value of 1 indicates no bias. All inundation coverage areas have units of km^2. *F*, *E*, and inundation coverage areas are also shown for the two sites tested using higher-resolution elevation data (MS-3m and NC-3m).

		AutoRoute + ARPP								AutoRoute + GISPP	
Location	Flow Rate	~~*F*~~	~~*E*~~	A_{Obs}	A_{Sim}	A_{Ove} r	A_{Unde} r	A_{Acc}	*F*	*E*	*F*	E
IN	Low	~~78.3~~	~~8.22~~	0.75	0.91	0.18	0.02	0.72	78.2	8.22	54.9	37.74
	Med	~~63.0~~	~~2.60~~	2.36	2.89	0.86	0.33	2.03	63.0	2.60	52.5	5.81
	High	~~81.7~~	~~0.11~~	5.48	4.66	0.10	0.92	4.56	81.7	0.11	78.4	0.54
CO	Low	~~63.1~~	~~0.70~~	0.71	0.66	0.13	0.18	0.53	63.1	0.70	53.1	3.19
	Med	~~62.2~~	~~0.15~~	2.68	1.89	0.14	0.93	1.75	62.2	0.15	59.0	2.04
	High	~~83.2~~	~~0.18~~	6.67	5.87	0.17	0.97	5.69	83.2	0.18	80.9	0.40
SC	Low	~~71.6~~	~~2.59~~	0.26	0.30	0.07	0.03	0.23	71.6	2.59	42.7	53.14
	Med	~~60.6~~	~~0.39~~	0.63	0.51	0.08	0.20	0.43	60.6	0.39	59.1	4.33
	High	~~65.9~~	~~0.12~~	0.97	0.70	0.04	0.31	0.66	65.9	0.12	75.8	1.41
NC	Low	~~39.3~~	~~10.97~~	3.65	7.82	4.58	0.42	3.23	39.3	10.97	27.7	15.43
	Med	~~92.6~~	~~1.32~~	20.27	20.48	0.89	0.67	19.60	92.6	1.32	87.0	1.55
	High	~~87.7~~	~~0.15~~	25.69	23.34	0.43	2.78	22.91	87.7	0.15	86.5	0.31
MS	Low	~~46.1~~	~~3.49~~	6.45	9.78	4.66	1.33	5.12	46.1	3.49	42.2	4.91
	Med	~~67.6~~	~~0.49~~	14.40	12.59	1.71	3.52	10.88	67.6	0.49	65.9	0.80

Deleted Cells
Deleted Cells
Inserted Cells
Inserted Cells
Inserted Cells
Inserted Cells

	High	70.2	0.20	21.46	16.98	1.13	5.61	15.85	70.2	0.20	68.9	0.60
MC	Low	80.0	2.62	1.26	1.39	0.21	0.08	1.18	80.0	2.62	57.3	24.96
	Med	76.7	2.10	2.18	2.39	0.41	0.19	1.99	76.7	2.10	57.9	6.31
	High	80.0	2.25	3.42	3.73	0.55	0.25	3.18	80.0	2.25	67.1	6.95
MW	Low	65.0	1.02	1.76	1.77	0.38	0.37	1.39	65.0	1.02	43.0	8.97
	Med	67.5	0.09	6.91	4.97	0.19	2.12	4.79	67.5	0.09	78.3	1.14
	High	74.0	0.17	8.57	6.93	0.34	1.98	6.59	74.0	0.17	83.0	0.99
MS (3m) 3m	Low	45.2	0.55	6.45	5.18	1.56	2.83	3.62	45.2	0.55		
	Med	56.8	0.20	14.40	9.90	1.10	5.59	8.81	56.8	0.20		
	High	71.2	0.12	21.46	16.41	0.66	5.71	15.75	71.2	0.12		
NC (3m) 3m	Low	39.5	10.69	3.65	7.75	4.53	0.42	3.23	39.5	10.69		
	Med	93.5	1.86	20.27	20.68	0.90	0.48	19.79	93.5	1.86		
	High	88.0	0.15	25.69	23.39	0.42	2.72	22.97	88.0	0.15		

745

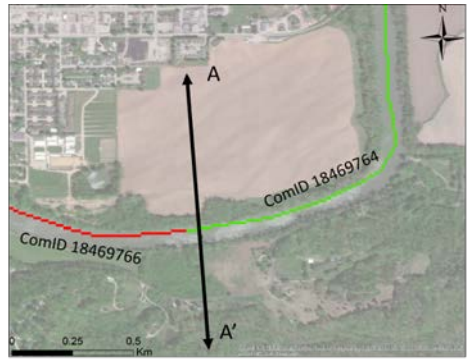
N
A
ComID 18469764
ComID 18469766
A'
0
0.25
0.5
Km

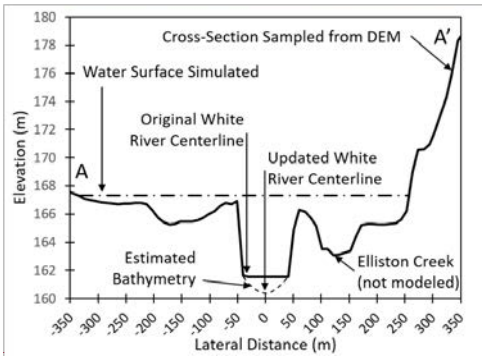
Cross-Section Sampled from DEM
A'
Water Surface Simulated
Original White
River Centerline
Updated White
River Centerline
A
Estimated
Bathymetry
Elliston Creek
(not modeled)
Elevation (m)
180
178
176
174
172
170
168
166
164
162
160
-350
-300
-250
-200
-150
-100
-50
0
50
100
150
200
250
300
350
Lateral Distance (m)

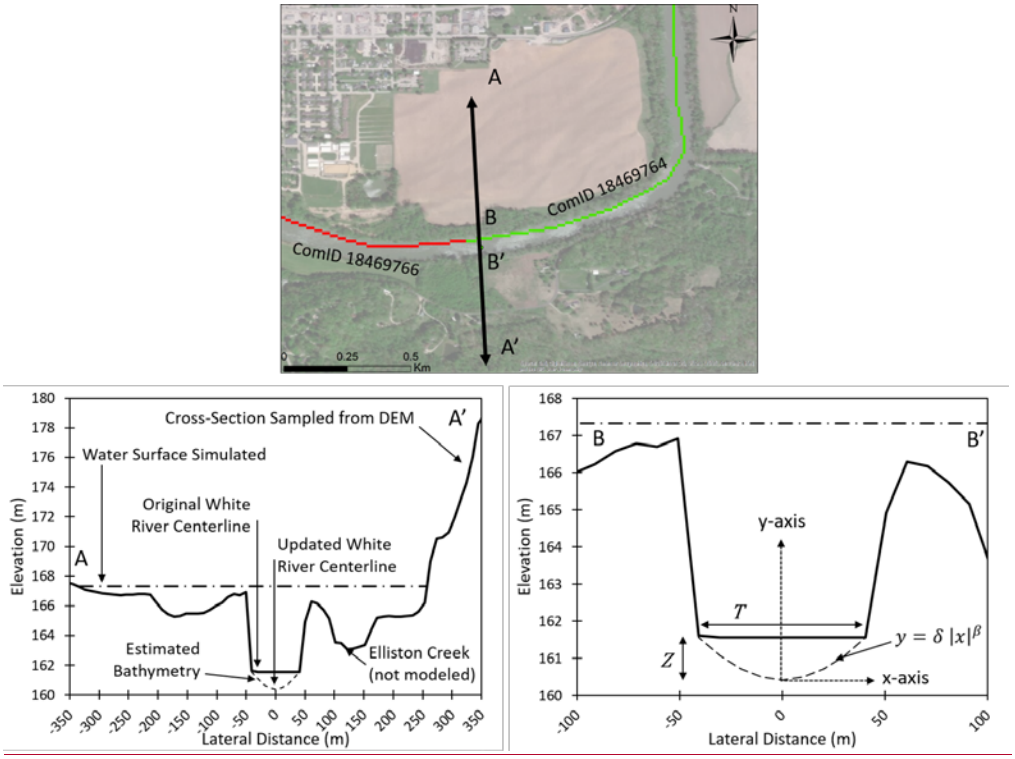

Figure 1: Cross-section profile of the White River near Spencer, IN. Also shown is the bathymetry estimation where T is the top-width of the channel, Z is the maximum depth of the bathymetry profile, and y and x are the ordinates of the bathymetry profile. **Sources of the background imagery in Figures 1-~~7~~3 and 5-9 include ESRI, DigitalGlobe, Earthstar Geographics, CNES/Airbus DS, GeoEye, USDA FSA, USGS, Getmapping, Aerogrid, IGN, IGP, and the GIS User Community.**

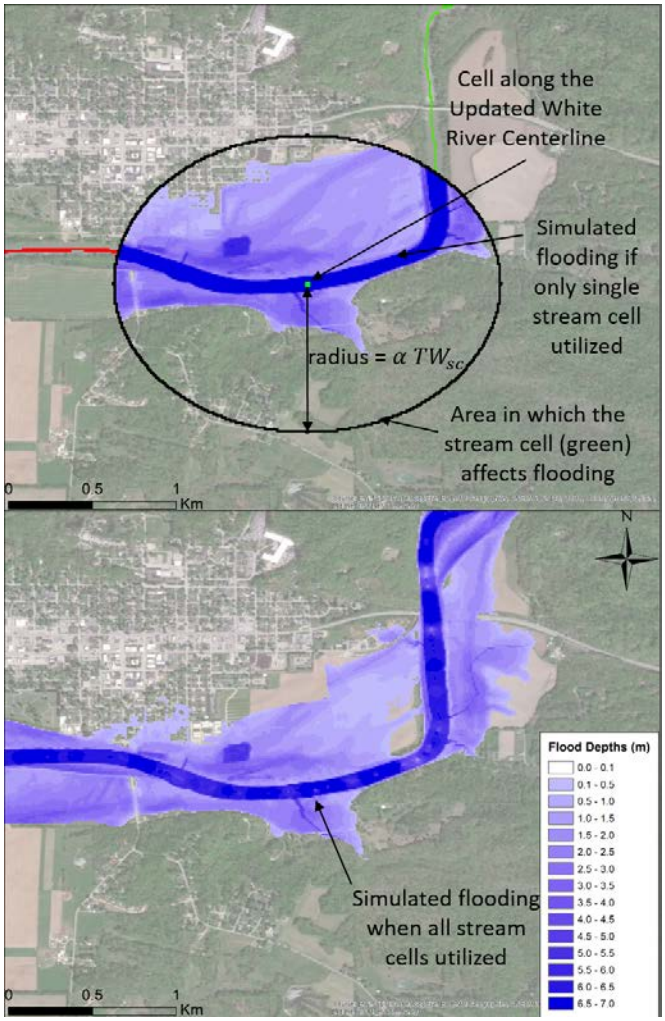

Figure 2: Top shows flood depths of surrounding terrain from at a single stream cell. Notice the area of influence (cells within radius=$\alpha\ TW_{sc}$) appears elliptical due to projection of the map. Bottom shows flood depths along the river when the depth from all stream cells are utilized. Notice that some areas shown as flooded in top figure are not flooded in bottom figure due to the influence of stream cells with lower depth calculations.

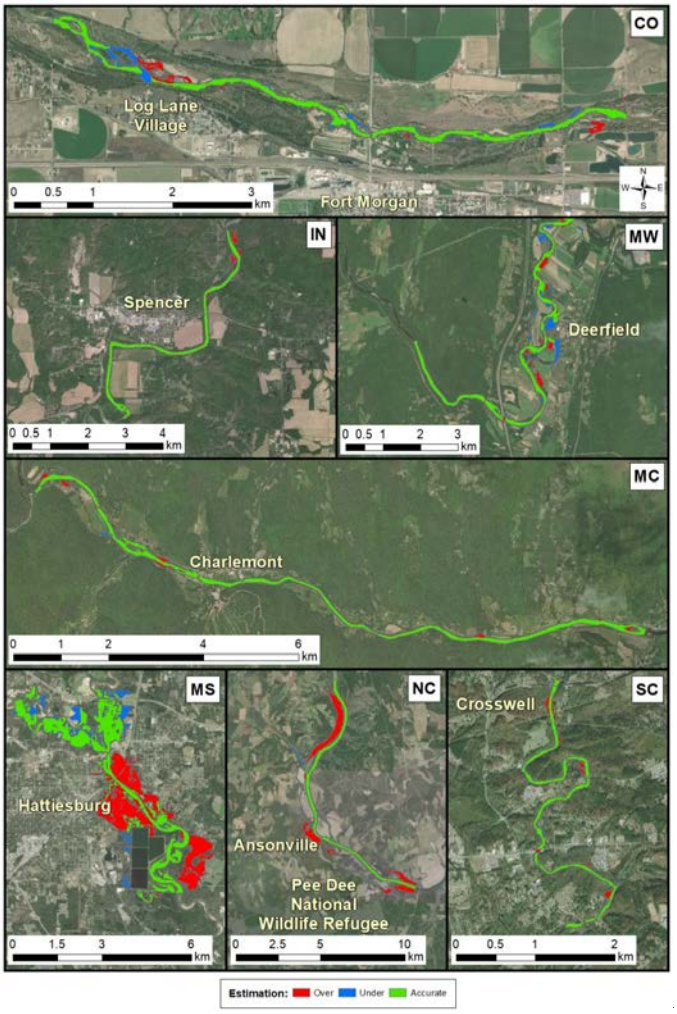
CO
Log Lane Village
Fort Morgan
0 0.5 1 2 3 km
N
W E
S
IN
Spencer
0 0.5 1 2 3 4 km
MW
Deerfield
0 0.5 1 2 3 km
MC
Charlemont
0 1 2 4 6 km
MS
Hattiesburg
0 1.5 3 6 km
NC
Ansonville
Pee Dee National Wildlife Refugee
0 2.5 5 10 km
SC
Crosswell
0 0.5 1 2 km
Estimation: Over Under Accurate

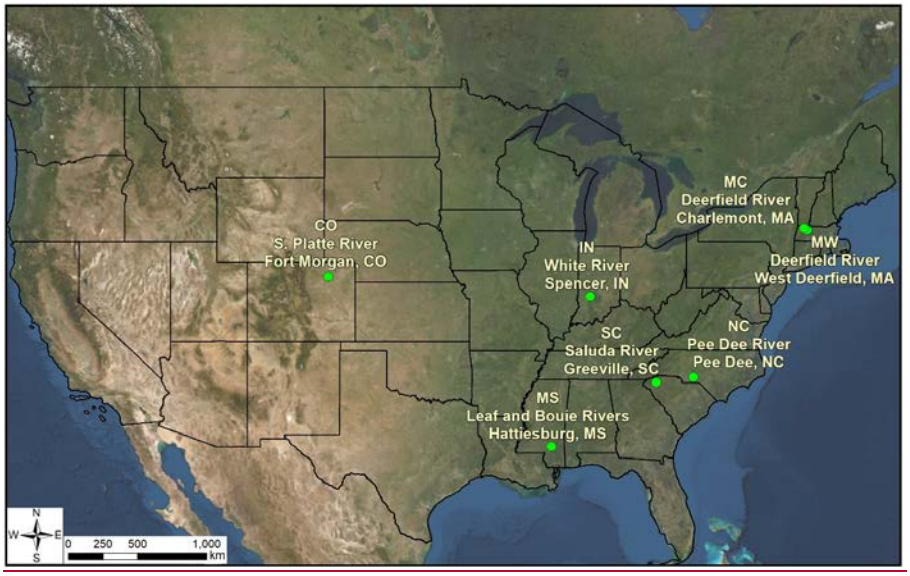

Figure 3: USGS study sites used in this study. For each study site the location, ID, and river(s) are provided.

765

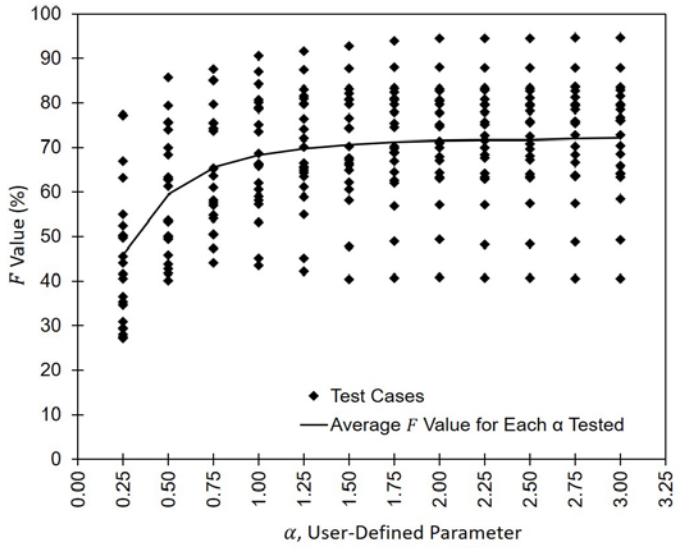

Figure 4: Sensitivity analysis of the user-defined parameter α, which controls the influence that each stream cell has on flooding the surrounding cells when using ARPP post-processing. F-statistic (F, percentage) values calculated using the observed and simulated flood inundation areas are plotted against the α value used in the simulation. In total, 252 simulations are shown (seven test sites, three flow scenarios, and twelve α values).

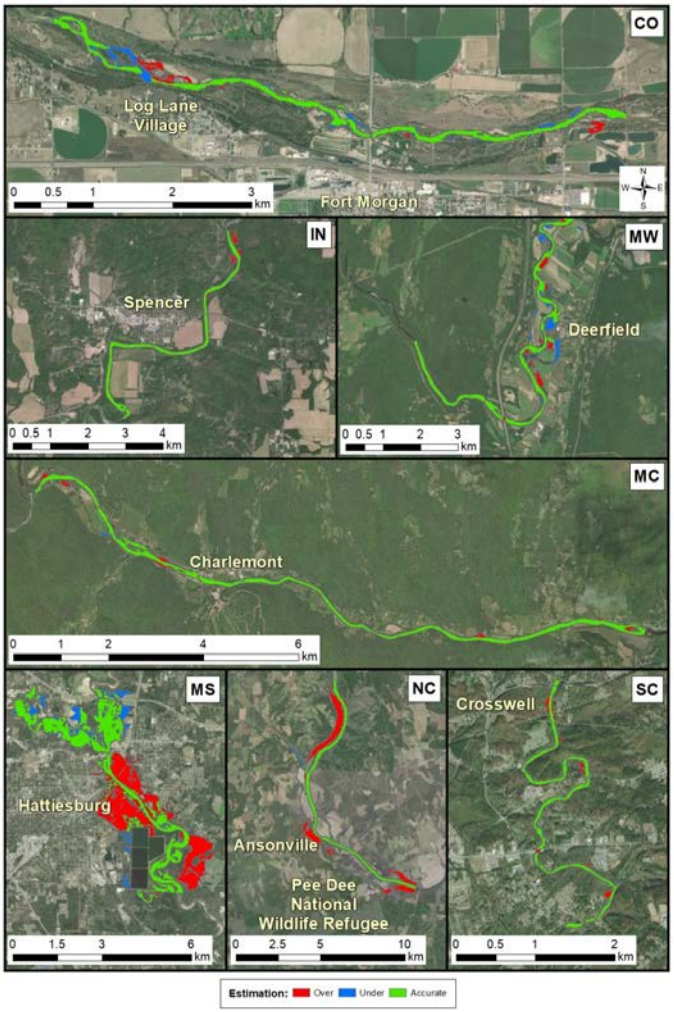

Figure 5: Flood map comparison between AutoRoute+ARPP simulations and USGS flood maps for low flow events at the seven test sites. Areas shaded green (Accurate) indicate areas where AutoRoute+ARPP and the USGS flood maps agree. Areas shaded red (Over) indicate where only AutoRoute+ARPP simulates the area as flooded. Areas shaded blue (Under) indicate where only the USGS shows the area as flooded.

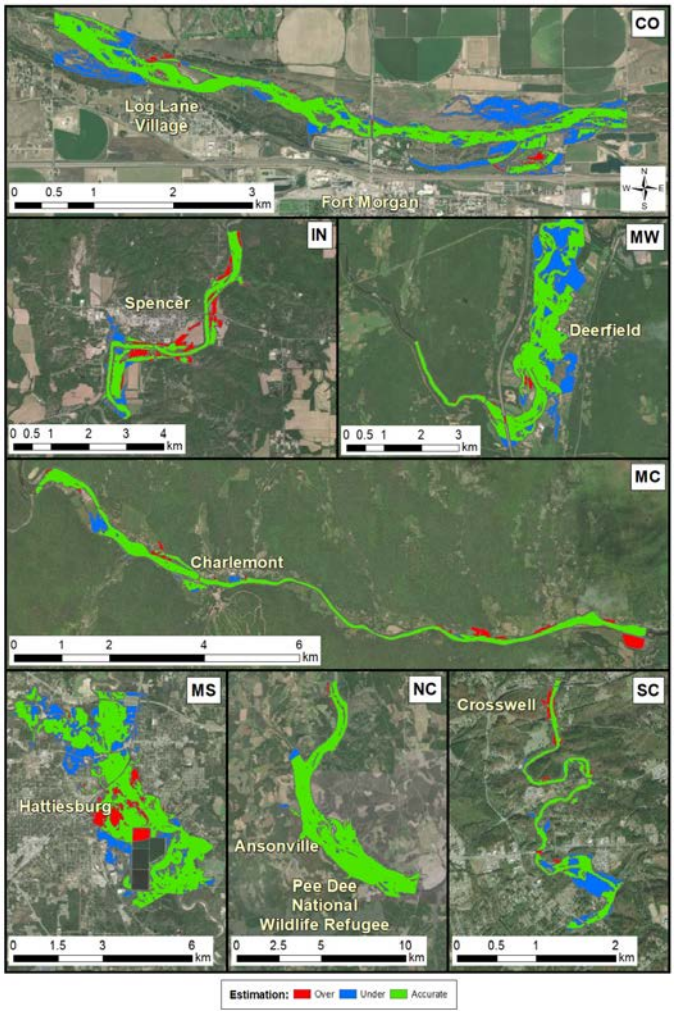

Figure 46: Flood map comparison between AutoRoute+ARPP simulations and USGS flood maps for medium flow events at the seven test sites. Areas shaded green (Accurate) indicate areas where AutoRoute+ARPP and the USGS flood maps agree. Areas shaded red (Over) indicate where only AutoRoute+ARPP simulates the area as flooded. Areas shaded blue (Under) indicate where only the USGS shows the area as flooded.

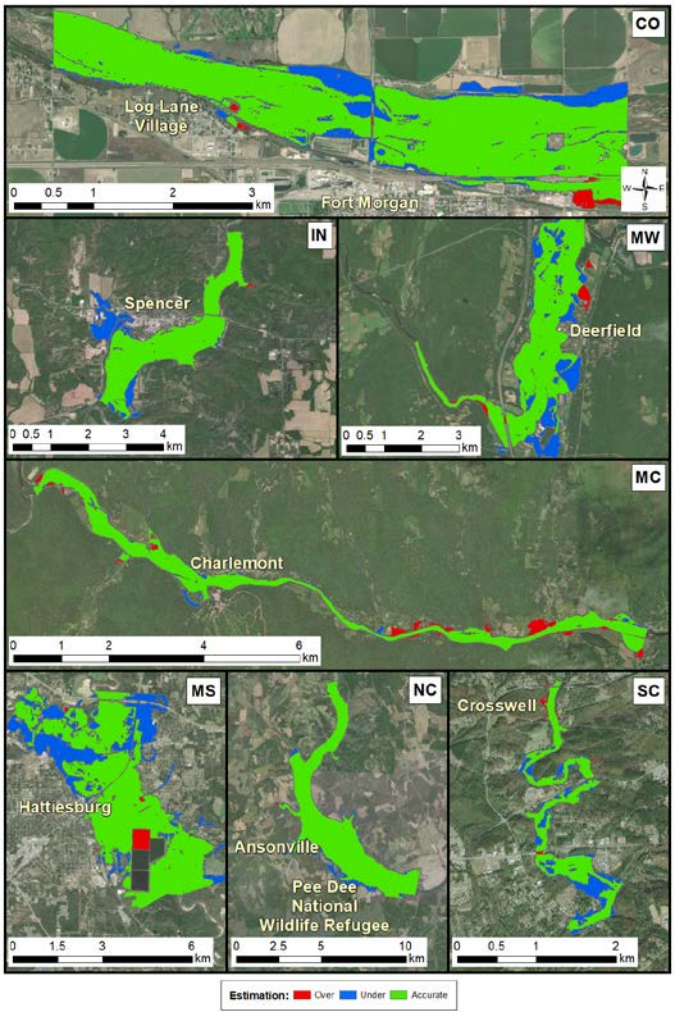

Figure 57: Flood map comparison between AutoRoute+ARPP simulations and USGS flood maps for high flow events at the seven test sites. Areas shaded green (Accurate) indicate areas where AutoRoute+ARPP and the USGS flood maps agree. Areas shaded red (Over) indicate where only AutoRoute+ARPP simulates the area as flooded. Areas shaded blue (Under) indicate where only the USGS shows the area as flooded. Some of the overestimation in the MS model simulation occurs at water treatment ponds, which were not included in the USGS flood maps and can bias the results.

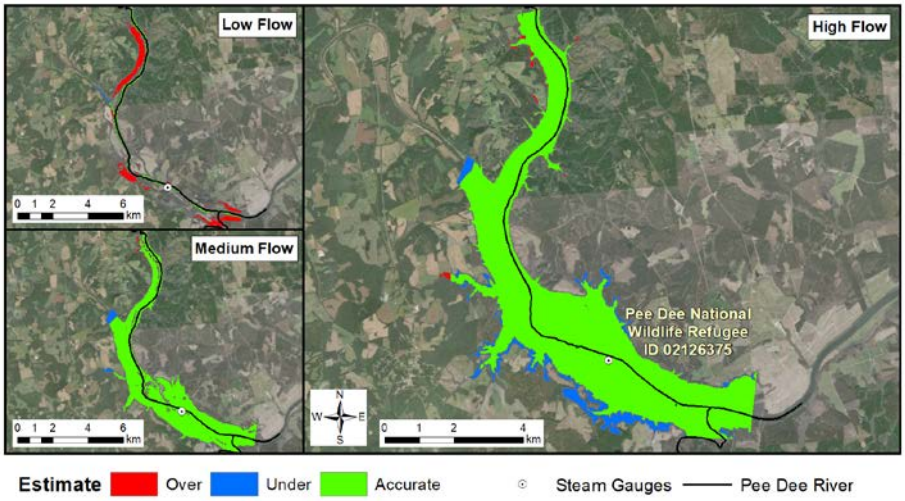

Figure 68: Pee Dee, NC (NC-3m) flood map comparison between AutoRoute+ARPP simulations using ~3 m DEM and USGS flood maps. Areas shaded green (Accurate) indicate areas where AutoRoute+ARPP and the USGS flood maps agree. Areas shaded red (Over) indicate where only AutoRoute+ARPP simulates the area as flooded. Areas shaded blue (Under) indicate where only the USGS shows the area as flooded.

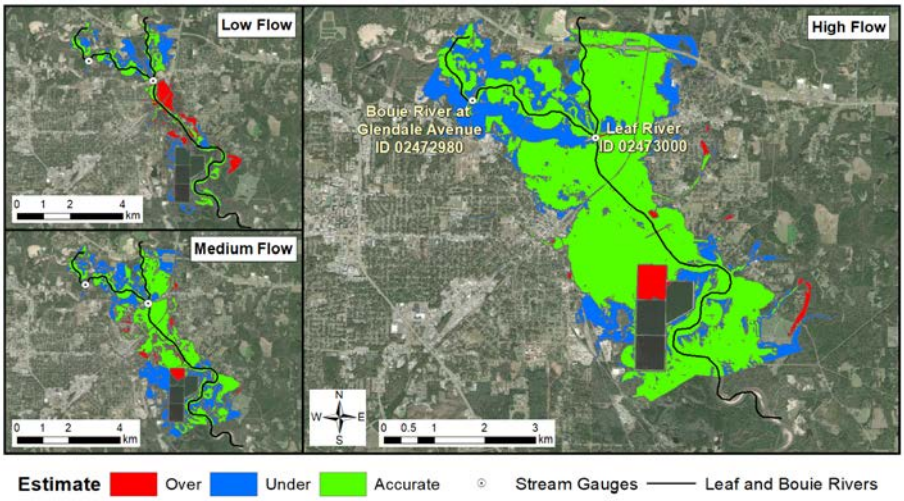

Figure 79: Hattiesburg, MS (MS-3m) flood map comparison between AutoRoute+ARPP simulations using ~3 m DEM and USGS flood maps. Areas shaded green (Accurate) indicate areas where AutoRoute+ARPP and the USGS flood maps agree. Areas shaded red (Over) indicate where only AutoRoute+ARPP simulates the area as flooded. Areas shaded blue (Under) indicate where only the USGS shows the area as flooded. Some of the overestimation in the model simulation occurs at water treatment ponds, which were not included in the USGS flood maps and can bias the results.